

2000

New Buffer Layers, Large Band Gap Ternary Compounds: CuAlTe^2

K. Benchouk

E. Benseddik

C. O. El Moctar

J. C. Bernède

S. Marsillac

Old Dominion University, Smarsill@odu.edu

See next page for additional authors

Follow this and additional works at: https://digitalcommons.odu.edu/ece_fac_pubs

Part of the [Electronic Devices and Semiconductor Manufacturing Commons](#)

Repository Citation

Benchouk, K.; Benseddik, E.; El Moctar, C. O.; Bernède, J. C.; Marsillac, S.; Pouzet, J.; and Khellil, A, "New Buffer Layers, Large Band Gap Ternary Compounds: CuAlTe^2 " (2000). *Electrical & Computer Engineering Faculty Publications*. 213.
https://digitalcommons.odu.edu/ece_fac_pubs/213

Original Publication Citation

Benchouk, K., Benseddik, E., El Moctar, C. O., Bernède, J. C., Marsillac, S., Pouzet, J., & Khellil, A. (2000). New buffer layers, large band gap ternary compounds: CuAlTe^2 *European Physical Journal: Applied Physics*, 10(1), 9-14. doi:10.1051/epjap:2000114

Authors

K. Benchouk, E. Benseddik, C. O. El Moctar, J. C. Bernède, S. Marsillac, J. Pouzet, and A Khellil

New buffer layers, large band gap ternary compounds: CuAlTe_2

K. Benchouk¹, E. Benseddik², C.O. El Moctar³, J.C. Bernède^{3,a}, S. Marsillac³, J. Pouzet³, and A. Khellil¹

¹ Université d'Oran, Laboratoire de Physique des Matériaux et Composants pour l'Électronique, B.P. 1524, El Mnaouer Oran, Algeria

² Université de Cadi Ayyad, Faculté des Sciences et Technique, B.P. 618, Guéliz, Marrakech, Morocco

³ Université de Nantes, Équipe de Physique des Solides pour l'Électronique, Groupe couche minces et Matériaux nouveaux, FSTN, 2 rue de la Houssinière, B.P. 92208, 44322 Nantes Cedex 03, France

Received: 10 September 1998 / Revised: 4 November 1999 / Accepted: 20 January 2000

Abstract. After deposition, by evaporation under vacuum, of Al/Cu/Te. multilayer structures, annealing at 673 K or more for half an hour, under argon flow, allows CuAlTe_2 films crystallised in the chalcopyrite structure to be obtained. The optical and electrical properties are interpreted by introducing the influence of impurity foreign phases present in the films. The optical properties are sensitive to the small Al_2O_3 domains randomly distributed into the CuAlTe_2 polycrystalline matrix. The optical band gap is slightly increased (2.35 eV) by the presence of alumina. The conductivity measurements show that a short circuit effect can be induced by a binary Cu_{2-x}Te degenerate phase present at the surface of the films. This effect can be suppressed by KCN etching of the samples that allows the superficial foreign phase to be dissolved.

PACS. 68.55.Jk Structure and morphology; thickness – 81.15.Ef Vacuum deposition

1 Introduction

I-III-VI₂ chalcopyrites have received serious attention as attractive candidates for active layers in polycrystalline thin films [1,2]. The production of efficient devices based on $\text{Cu}(\text{In,Ga})\text{Se}_2$ film as an absorber, has been tied closely with the use of CdS windows [3]. The CdS is deposited by chemical bath deposition. However, while this technique provides conformal coverage of the absorber semiconductor, it is not suitable for industrial processes. Moreover, the use of cadmium raises the apprehension of consumers for ecological reasons.

Therefore, elimination of CdS is viewed as a major contribution to reducing the negative environmental perception of technology. One possibility is to substitute for CdS another thin film with similar properties (band gap ≈ 2.5 eV, *n* and *p* types of material accessible, lattice matching with $\text{Cu}(\text{In,Ga})\text{Se}_2$, stability, etc.).

In the ternary I-III-VI₂ family, CuAlX_2 appear as good candidates for buffer layers in $\text{Cu}(\text{In,Ga})\text{Se}_2$ based solar cells. They have the same chalcopyrite structure, their band gap varies from 2 eV ($X = \text{Te}$) to 3.5 eV ($X = \text{S}$) and they can be either *p* or *n* type. We have shown earlier [4] that CuAlTe_2 films can be obtained by post-annealing under argon flow of $\text{Cu}/\text{Al}/\text{Te}/\text{Al} \dots \text{Cu}/\text{Al}/\text{Te}$ sequentially deposited structures.

In this paper, after checking the quality of the films by X-ray diffraction, scanning electron microscopy and

microprobe analysis, they are optically and electrically characterized. It is shown that an upper binary compound (Cu_{2-x}Te) layer is present at the surface of the film. After removing this layer by a KCN treatment, as expected, the films behave like a semiconductor with a large band gap, as expected.

2 Experimental technique

The process used to achieve CuAlTe_2 films has been described earlier [4], it will only be briefly recalled here. The films were sequentially deposited on soda lime glass in vacuum (5×10^{-5} Pa) by thermal evaporation from three tungsten crucibles to give $\text{Cu}/\text{Al}/\text{Te}/\text{Al} \dots \text{Cu}/\text{Al}/\text{Te}$ layers. The CuAlTe_2 films were synthesised by reaction between the constituents during a half hour post-annealing under argon flow. The evaporation rates and layer thicknesses were measured *in situ* by the vibration quartz method. The thickness of the thin layers of the constituents were calculated in order to achieve the desired composition. The total thickness was 1 μm .

The quality of the films was checked by X-ray diffraction (XRD), scanning electron microscopy (SEM) and microprobe analysis. Then the CuAlTe_2 films were characterized electrically and optically. The absorption coefficient of the films has been deduced from the transmission of two samples with different thicknesses [5], while conductivity measurements were done after gold electrode deposition on planar samples.

^a e-mail:

jean-christian.berne@physique.univ-nantes.fr

The optical measurements were carried out at room temperature using a Cary 2300 spectrophotometer. The optical density (O.D) was measured at wavelengths 2–0.5 μm^1 . For electrical measurements, gold electrodes were evaporated after the deposition of the thin films. Gold was selected because it gives a good ohmic contact. The films' dc conductivity was measured with an electrometer between 100 K and 500 K.

3 Experimental results

3.1 Film quality

We have shown in an earlier paper [4] that the optimum annealing time is half an hour. Therefore all the films studied in the present work have been annealed for half an hour.

The microprobe analysis showed that the films could be strongly contaminated by oxygen (up to 40 at.%) during the deposition process. Therefore, while the deposition rate of aluminium has been increased up to 1 nm/min, the deposited aluminium films were immediately covered with a chalcogene layer in order to prevent oxide formation. By using such a process, the relative atomic concentration of oxygen present in the films at the end of the deposition was decreased to 8 at.%, whatever the annealing temperature (673 or 773 K).

The typical thin film composition of a good film is: Te 46 at.%, Cu 21 at.%, Al 24 at.% and oxygen 9 at.%. The small aluminium excess is bonded to oxygen to give Al_2O_3 amorphous micro-domains randomly distributed in a CuAlTe_2 (Fig. 1) polycrystalline matrix. The presence of some Al_2O_3 in the films with the deposition conditions used is probable as shown by Kim *et al.* [4]. However, since a careful observation of the DRX diagram does not indicate the presence of an amorphous phase, Al_2O_3 should be present in the films in very small domains, it may accumulate at the grain boundaries. Moreover, some oxygen can be substituted to some Te in the CuAlTe_2 and can also be intercalated.

If it can be seen that there are neither pinholes nor cracks in the films (Fig. 2a), the visualisation of the films with higher magnification shows that they are polycrystalline. Some large crystallites are randomly distributed onto the films (Fig. 2b). It can be seen by microprobe analysis that they can be attributed to some Cu_{2-x}Te compound.

The average grain size in the polycrystalline matrix is about 50–100 nm while the superficial binary compound micro-crystallites are larger (100–300 nm). The binary compound, can be etched by KCN solution. The KCN concentration used is 0.1 M. After etching (Fig. 2c), while the broad binary crystallites have disappeared, the surface of the films appears quite rough. The presence of Cu_{2-x}Te binary compound before etching is also visible in the XRD diagrams (Fig. 1). The cross-section of films (Fig. 3) shows

¹ Optical measurement have been carried out at the LPC IMN.

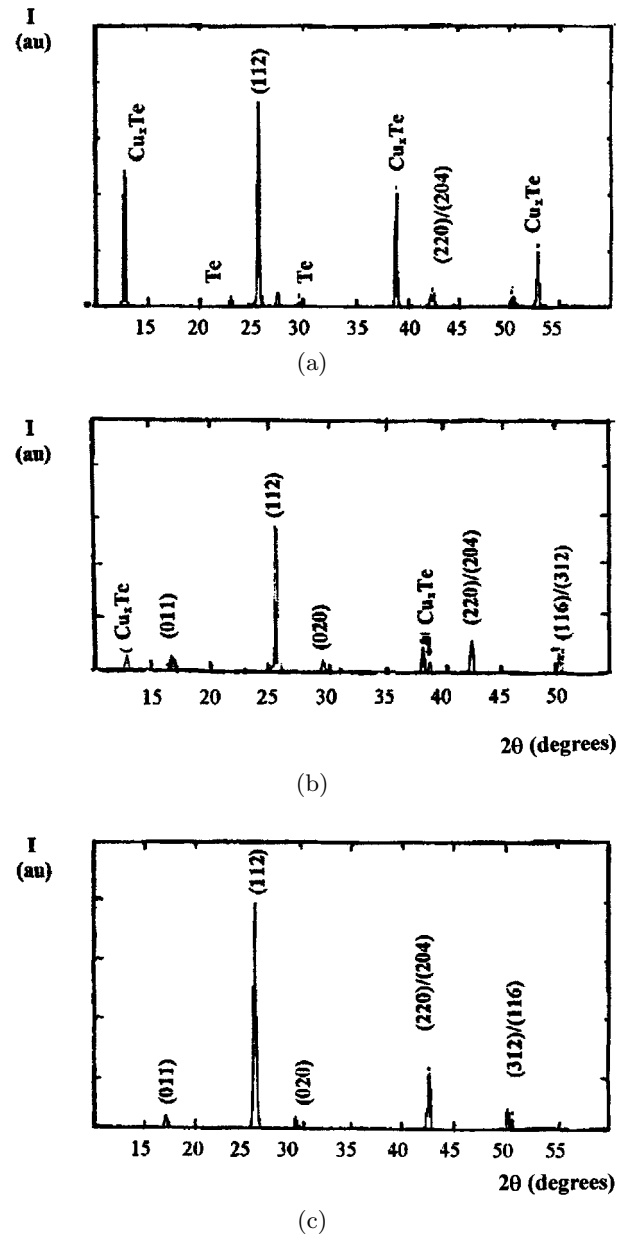


Fig. 1. X-ray diffraction diagrams of 1 μm thick CuAlTe_2 films (λ Cu $K\alpha = 0.153406$ nm-peaks labeled are CuAlTe_2); (a) annealed for half an hour at 773 K, (b) annealed for half an hour at 673 K, (c) after removing the Cu_xTe phase by etching in KCN.

that only small crystallites, typical of the CuAlTe_2 compound, are visible in the bulk, which confirms that the binary is only present at the surface of the films.

Figure 1a shows the X-ray diagram of a 1 μm thick film after annealing at 773 K, whereas Figure 1b is the diagram obtained from a sample deposited in the same run but annealed at 673 K. It can be seen that these temperatures allow one to obtain well-crystallised CuAlTe_2 films. If the peak intensity increases with the annealing temperature, the amount of binary phase also increases.

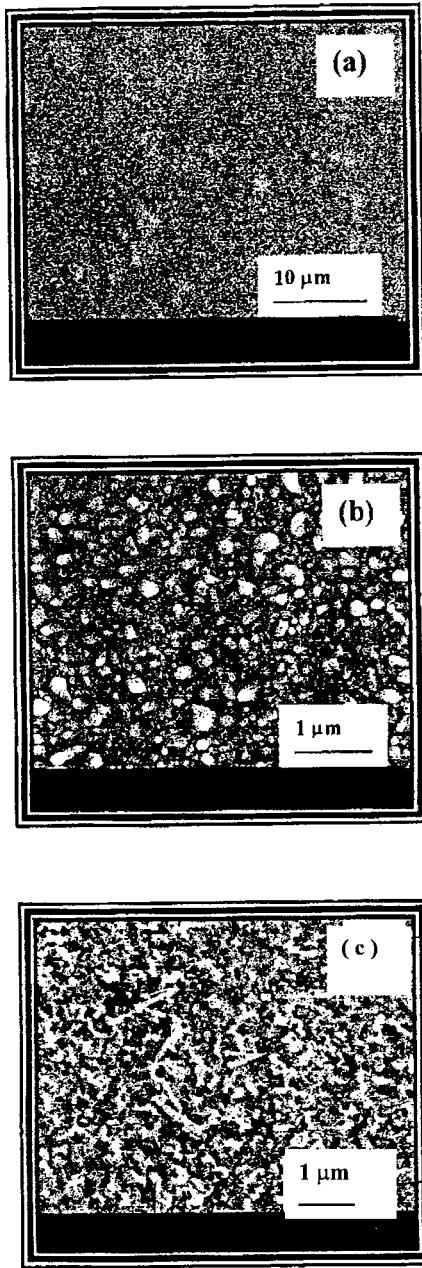


Fig. 2. Micrograph of a 1 μm thick CuAlTe₂ film; (a) small magnification, (b) large magnification, (c) “after KCN” etching 1 min in 0.1 M KCN.

This result is in good agreement with earlier results [4]. After a half hour annealing at 673 K, as usual for chalcopyrite compounds such as CuInSe₂ [7], the (112) peak dominates, which shows that the crystallites of the films are oriented along the (112) direction. Moreover, the (101) and (103) peaks typical of the chalcopyrite structure are visible (Fig. 1). Therefore, CuAlX₂ films crystallised in the chalcopyrite structure have been synthesised using the technique described above.

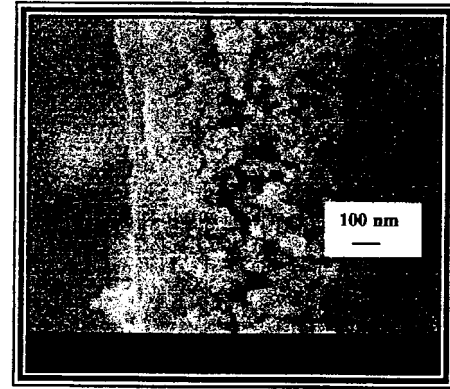


Fig. 3. Micrograph of a cross-section of a CuAlTe₂ film.

The CuAlTe₂ crystallises in the D¹² space group with $a = 5.964 \text{ \AA}$ $c = 11.975 \text{ \AA}$ [8]. When these parameters are calculated from the inter-planar spacing measured by XRD, it can be seen that there is a small increase of the lattice parameters: $a = 6.042 \text{ \AA}$ and $c = 11.975 \text{ \AA}$. As discussed earlier, some oxygen can be substituted for selenium and intercalated in the films. With the oxygen size being smaller than that of tellurium, a decrease of the lattice parameter should be expected in the case of substitution, however, some oxygen can be also intercalated; in that case [9] the structural unit would increase, which is the present case. Therefore, there is probably some intercalation effect during the crystallisation process of the film.

3.2 Optical and electrical characterisation

All the films studied below were annealed for half an hour at 673 K. The absorption coefficients α were calculated from the measured transmission $T(\log(1/T) = \text{O.D (optical density)})$ of two samples with different thicknesses:

$$\alpha = \frac{1}{t_2 - t_1} \log \frac{T_1}{T_2}.$$

Where t is the thickness of the film. The plot of $(\alpha h\nu)^2$ *vs.* the photon energy is reported in Figure 4. The direct optical band gap deduced from the high absorption domain is 2.3 eV. It should be noted that some absorption subsists below the threshold energy value, which will be discussed below.

In Figure 5 we show the conductivity, σ , of a typical film in an Arrhenius plot ($\log \sigma$ *vs.* $10^3/T$). It can be seen that before etching (Fig. 5a), σ increases with the temperature, however the activation energy is relatively weak even in the high temperature domain. This behaviour is not expected for a semiconductor with quite a large band gap. The room temperature conductivity is very high ($\sigma_{300\text{K}} = 10 \Omega^{-1} \text{ cm}^{-1}$); this is the behaviour of a degenerated semiconductor rather than a classical semiconductor.

We have shown above that on the surface of the films there is a Cu_{2-x}Te impurity phase that is highly

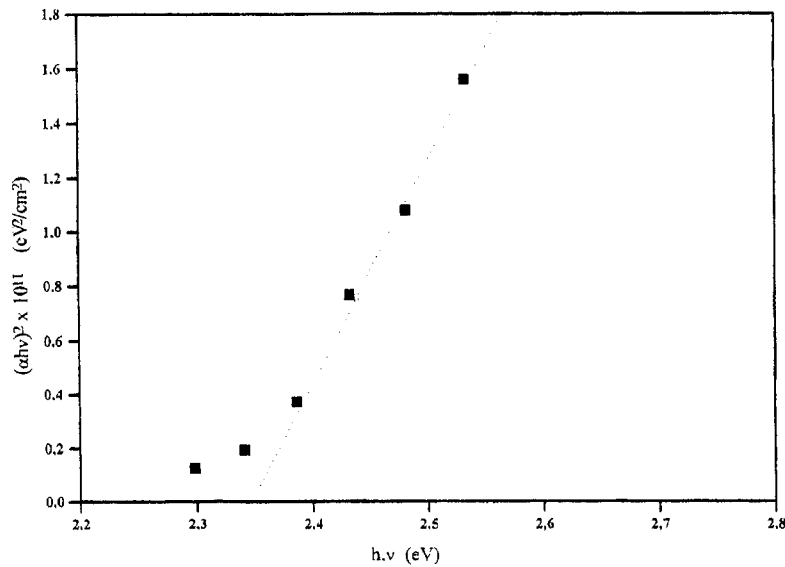


Fig. 4. Curve of $(\alpha h\nu)^2$ versus energy.

conductive. After removal of this phase by treatment in a KCN solution the results are significantly different (Fig. 5b). The conductivity at room temperature was $10^{-1} \Omega^{-1} \text{cm}^{-1}$. It was possible to measure a variation in the conductivity of over two orders magnitude in the temperature domain 160–500 K.

4 Discussion

The results of the optical and electrical measurements will be discussed below in the light of the physicochemical characterisation of the films. XRD diagrams have shown that the main phase present in the films is CuAlTe_2 with a chalcopyrite structure. However, it has been shown by microprobe analysis that some oxygen is systematically present in the films (8 at.%). This oxygen contamination should be correlated to the measured tellurium and copper deficiency. If we consider that the aluminium excess is bonded to oxygen to form Al_2O_3 we can conclude that after KCN etching the films consist of a CuAlTe_2 polycrystalline matrix where an Al_2O_3 amorphous impurity is randomly distributed in small amounts. We have shown that the band gap deduced from density measurements is 2.35 eV which is sensibly higher than the usual value of 2.06 eV measured in CuAlTe_2 [10].

This small increase of the optical gap can be explained by the presence of the small Al_2O_3 domains randomly distributed in the CuAlTe_2 polycrystalline matrix. In a heterogeneous system we can assume that the sample can be divided into two phases. If N_{ternary} and N_{oxide} are the respective densities of the CuAlTe_2 and Al_2O_3 particles in the films, α the absorption coefficient, is assumed to be given by [11]:

$$\alpha = \frac{\alpha_{\text{CuAlTe}_2} N_{\text{CuAlTe}_2} + \alpha_{\text{oxide}} N_{\text{oxide}}}{N_{\text{CuAlTe}_2} + N_{\text{oxide}}}.$$

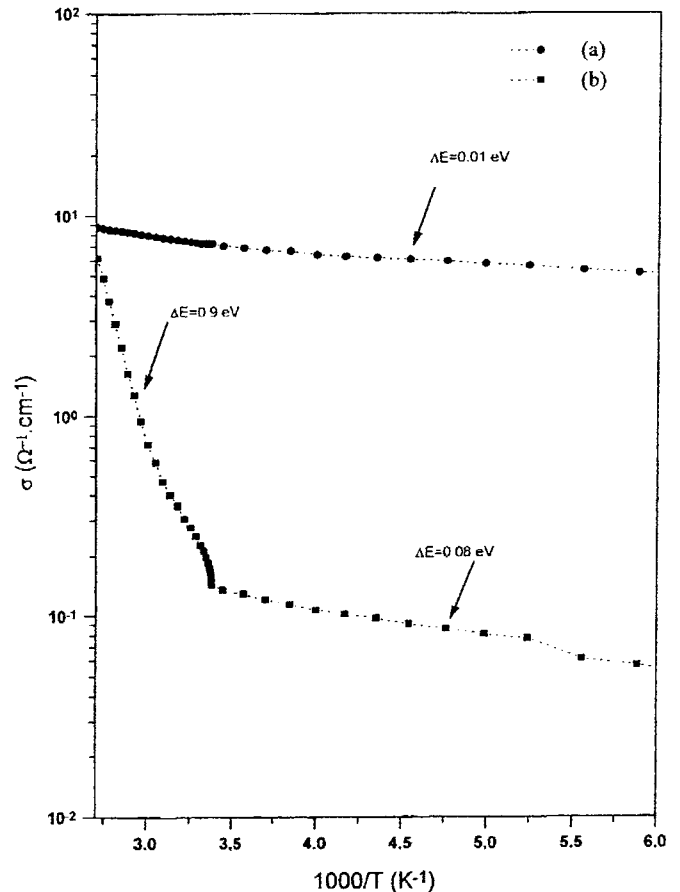


Fig. 5. Temperature dependance of the conductivity of CuAlTe_2 films versus the inverse of the temperature; (a) as annealed samples, (b) after removing the Cu_xTe phase by etching in KCN.

Table 1. Conductivity measurements.

CuAlSe ₂ film	Room temperature conductivity ($\Omega^{-1} \text{ cm}^{-1}$)	ΔE_1 (eV)	ΔE_2 (eV)
Before etching	10^1		0.01
After etching	10^{-1}	0.9	0.08

Where α_{CuAlX_2} and α_{oxide} are the absorption coefficients of the CuAlX₂ and oxide phase respectively. From the equation, α will depend on the absorption coefficient of the oxide phase and therefore on its optical band gap. Since the Al₂O₃ band gap ($E_g = 8.7$ eV) is greater than that of CuAlTe₂, ($E_{g\text{CuAlTe}_2} = 2.06$ eV) there will be some shift (ΔE_g) of the band gap [11]. The measured optical band gap will be larger than that expected for a pure chalcogenide compound.

However, as no amorphous phase is evidenced by XRD analysis, and since some oxygen may be substituted and intercalated in the CuAlTe₂ matrix, we can assume that the gap is also modified by the presence of oxygen. It has been shown by Hill [12] that the energy gap of a semiconductor alloy varies with its composition.

The main values deduced from the conductivity measurements are reported in Table 1. It can be seen from Table 1 and Figure 5 that before and after etching the films exhibit a very different behaviour. Before KCN etching, the near zero (0.01 eV) activation energy and the high room temperature conductivity should be attributed to the superficial Cu_{2-x}Te compound, a degenerate semiconductor. As observed by SEM, the binary compound is randomly distributed at the surface of the films. A percolation law such as that obtained by the fluctuation induced tunnelling conduction model in disordered materials [13] can explain the small activation of the conductivity with the reciprocal temperature.

After KCN etching, the room temperature conductivity and activation energy values are typical of inorganic semiconductors. It was possible to measure the conductivity increase by over two orders of magnitude. The resulting curve in the Arrhenius plot has linear points. At high temperature ($T > 350$ K) we can extract from the slope, an activation energy of 0.92 eV. At low temperature the activation energy is 0.08 eV.

Classically in the higher temperature domain, semi-conductivity follows the law:

$$\sigma = \sigma_0 \exp\left(-\frac{E_g}{2kT}\right)$$

with k being the Boltzmann constant.

Therefore from the measured activation energy (0.92 eV) we can estimate the electrical band gap at $E_0 = 1.82$ eV, this is slightly smaller than the expected optical band gap (2.06 eV). This small difference is probably related to the disorder present in the films, which induces band tail formation of localised states [14,15].

It has been shown that rather high sub-band gap absorption coefficients were observed for films containing

second phase particles. This absorption is present in our samples as shown in Figure 4. Probably, in the temperature range concerned here, the measured activation energy corresponds to carriers issued from localised states of the band tail to the band of extended states. In that case the conductivity is more precisely given by [16]:

$$\sigma = \sigma' \exp\left(-\frac{\Delta E'}{kT}\right).$$

With, in the case of p type conductivity, $\Delta E' = E_F - E_B = \Delta W$. Where ΔW is the hopping energy in the localised states, E_B is the energy limit of the band tail and E_F is the Fermi level.

Therefore, the presence of the band tail induced in the band gap could explain the small discrepancy between the expected band gap value and the values deduced from electrical measurements.

In the low temperature domain, the activation energy could be attributed to activation of carriers from an energy level introduced in the band gap by some defects/or impurities. Such ionisation energy (80 meV) has already been measured in these ternary compounds [17,18].

It should be noted that activation energies of about 80 meV have already been attributed to intrinsic defect levels such as vacancies and/or interstitial of the elements [14]. Another possibility is that the conductivity is governed by grain boundary scattering. For this case it has been shown [19] that

$$\sigma \approx \exp\left(-\frac{q\Phi_B}{kT}\right).$$

With Φ_B being the barrier height at the grain boundary. However, the room temperature conductivity is quite high, and not very different from the expected value for a single crystal. The temperature domain covered by the variation law giving $E = 80$ meV is very large; down to 300 K, which is quite unusual for such polycrystalline films [16].

5 Conclusion

It has been shown that CuAlTe₂ films can be obtained from Cu/Al/Te...multilayer structures after a half hour annealing at 673 K.

Some binary compound forms at the surface of the films, which strongly influences the conductivity of the films. After KCN etching the measured conductivity is mainly controlled by the CuAlTe₂ properties. The optical properties of the films are also modified by foreign contributions: the small Al₂O₃ domains randomly distributed

at the grain boundaries of the CuAlTe₂ films and/or some oxygen substitution and intercalation in the CuAlTe₂. The optical band gap deduced from experimental measurements of 2.35 eV, is slightly higher than that expected for pure material, which is promising for the use of these films as buffer layers in solar cells, since the CdS layer normally used, has a band gap of 2.45 eV.

This work was supported by a contract between France and Algeria (CMEP 00 MDU 510).

References

1. *14 European Photovoltaic Solar Energy Conference and Exhibition, Barcelona (Spain), 30 June-4 July 1997*, edited by H.S. Stephens and associates, Bedford, UK.
2. *2nd World Conference and Exhibition on Photovoltaic Solar Energy Conversion, Wien (Austria), 6-10 July 1998*, edited by H.S. Stephens and Associates, Bedford, UK.
3. Renewable & Sustainable, Energy Rev. Vol. 1, No. 1/2 (March/June, 1997).
4. K. Benchouk, C. El Moctar, J.C. Bernede, S. Marsillac, J. Pouzet, N. Barreau, M. Emziane, J. Mater. Sci. **34**, 1847 (1999).
5. A. Mallouky, J.C. Bernede, Thin Sol. Fi. **158**, 285 (1988).
6. J. Kim, J.J. Weimer, M. Zukic, D.G. Torr, J. Vac. Sci. Technol. A **12**, 3062 (1994).
7. D. Haneman, CRC Critical Rev. Solid State Mater. Sci. **14**, 377 (1988).
8. J.E. Jaffe, A. Zunger, Phys. Rev. B **29**, 1882 (1984).
9. T.K. Mandal, S.K. Srivastava, Mater. Chem. Phys. **47**, 283 (1997).
10. Sato Katsuaki, Denki Kagaku, Oyobi Kogyo, Butsuri Kagaku **56**, 228 (1988).
11. K. Toda, N. Tanino, T. Muria, Y.C. Liong, K. Furutine, Thin Sol. Fi. **108**, 293 (1983).
12. R.J. Hill, Phys. C. Solid State Phys. **7**, 521 (1979).
13. P. Sheng, Phys. Rev. B **21**, 2180 (1980).
14. J. Szot, U. Prinz, J. Appl. Phys. **66**, 12 (1989).
15. J.R. Tuttle, D. Albin, R.J. Matson, R. Noufi, J. Appl. Phys. **66**, 4408 (1989).
16. N.F. Mott, E.A. Davis, *Electronics Process in Non-crystalline Materials*, 2nd edn. (Clarendon Press-Oxford, 1979), p. 201.
17. F. Abou-Elfatouh, D.J. Dunlavy, T.J. Coutts, Solar Cells **27**, 237 (1989).
18. H.Y. Ueng, H.L. Hwang, J. Phys. **62**, 434 (1987).
19. J.Y. Seto, J. Appl. Phys. **12**, 5247 (1975).